

# Influence of Nanotube Chirality, Temperature, and Chemical Modification on the Interfacial Bonding between Carbon Nanotubes and Polyphenylacetylene

Huijuan Chen, Qingzhong Xue,\* Qingbin Zheng, Jie Xie, and Keyou Yan

College of Physics Science and Technology, China University of Petroleum, Dongying, Shandong 257061, People's Republic of China

Received: April 22, 2008; Revised Manuscript Received: August 06, 2008

Molecular dynamics (MD) simulations were used to study the interaction energy between single-walled carbon nanotubes (SWNTs) and polyphenylacetylene (PPA). The “wrapping” of nanotubes by PPA chains was computed. The influence of nanotube chirality, temperature, and chemical modification on the interfacial adhesion of nanotube–PPA was investigated. The results showed that the interaction energy between the SWNTs and PPA is strongly influenced by chirality but the influence by temperature could be negligible. For SWNTs with similar molecular weights, diameters, and lengths, the armchair-type nanotube may be the best nanotube for reinforcement. Besides, our simulations indicated that some specific chemical modifications of SWNTs play a very important role in determining the strength of interaction between the SWNTs and PPA. The SWNTs modified by methyl or phenyl groups can be well-wrapped by PPA, while the SWNTs modified by other types of groups cannot. The results also indicated that the interaction energy between the SWNTs and PPA increases with the increase of the concentration of functionalized groups. People have demonstrated that the increase of the concentration of functionalized groups can weaken the mechanics of SWNT. Therefore, the attachment of methyl or phenyl groups with reasonable concentration to the outer SWNTs should significantly improve the load transfer between the SWNTs and polymer when the SWNTs are used to produce nanocomposites.

## 1. Introduction

Carbon nanotubes (CNTs), containing long, thin cylinders of carbon with multiple wall layers, were first discovered by Iijima in 1991<sup>1</sup> and later found as single-wall structures. CNTs have attracted great research interest due to their unique properties, such as high electrical and superlative mechanical properties. In particular, this combination of properties makes them ideal candidates as nanofibers to enhance the properties of composites. Using CNTs as nanofibers to enhance the properties of composite materials has been explored extensively both in experimental and theoretical studies. Recent experiments have shown that the addition of small amounts of CNTs to polymers can change some selective material properties such as mechanical<sup>2–6</sup> and electrical,<sup>7,8</sup> thermal,<sup>9–11</sup> and optical<sup>12</sup> properties. However, there was another report about the morphology analysis of fracture surface of CNT–epoxy composites by Bower et al.<sup>13</sup> Their results suggested that no broken CNTs were observed. It indicated that the load transfer from polymer to CNTs was not sufficient to fracture the CNTs because the CNTs tend not to bond strongly with their host matrix. To take advantage of the awfully high Young's modulus and strength of CNTs, an efficient load transfer from the polymer matrix to the CNTs is required. Therefore, another significantly challenging issue is the interfacial bonding between the nanotubes and polymer matrix, which determines the efficiency of load transfer from the polymer matrix to the CNTs.<sup>14</sup>

To improve the interfacial bonding between CNTs and polymer matrix, it is a possible way to add chemically functionalized CNTs into the matrix. There are some experimental reports about investigations of the functionalized

CNTs,<sup>15–17</sup> and Kuzmany et al.<sup>15</sup> have reported that an efficient way to render the CNTs soluble either in aqueous or organic phase is by attaching different functional groups (–OH, –COOH, –F) directly to CNTs and using substitution reactions to change these simple groups formed. In this study, we take four kind of groups (–OH, –F, –CH<sub>3</sub>, –C<sub>6</sub>H<sub>5</sub>) into account.

However, it is difficult to study the CNT–polymer interface by experimental methods. Recently, molecular mechanics (MM) and molecular dynamics (MD) simulations have become increasingly popular in the investigations of reinforcement mechanisms in CNT–polymer composite systems. Yang et al.<sup>18</sup> have studied the interactions between polymer and CNTs by MD simulation. They found that the specific monomer structure plays a very important role in determining the strength of interaction between nanotubes and polymer. Gou et al.<sup>19</sup> used MM and MD simulations to study the molecular interaction and load transfer in the presence of single-walled carbon nanotube (SWNT) rope. The simulations showed that individual nanotubes have stronger interactions with the epoxy resins than the nanotubes rope. Frankland et al.<sup>20</sup> had investigated the influence of chemical cross-links between a SWNT and a polymer matrix on the matrix–nanotube shear strength by MD simulations. The results suggested that load transfer and modulus of nanotube–polymer composites can be effectively increased by deliberately adding chemical cross-linking. Few investigations about the influence of chemical attachment on interfacial properties of CNTs have been reported. This study focused on finding a better way to get CNTs to interact well with other materials. The method pursued here for making CNTs capable of effectively interacting with polymer was based on the covalent attachment of functional groups to the surface of CNTs. By taking advantage of these functional groups, which could act as effective interfacial bridges between the CNTs and the polymer

\* To whom correspondence should be addressed. E-mail: xueqingzhong@tsinghua.org.cn. Phone: +86-546-8392123. Fax: +86-546-8392123.

matrix, an effective load transfer could be achieved between the CNTs and the polymer matrix. In this study, the influence of nanotube chirality, temperature, and some specific chemical modifications on the interfacial bonding between the SWNTs and polyphenylacetylene (PPA) was investigated using MM and MD simulations.

## 2. Experimental Section

**2.1. Computational Method and Force Field.** In this research, MD simulations were conducted to explore the interaction between SWNTs and PPA. The wetting properties of the SWNTs and PPA were also studied using the MD simulations, which can provide us with some useful information for the development of nanotube-based polymeric composites. Here, MD simulations were carried out through a commercial software package called Materials Studio developed by Accelrys Inc. The condensed phase optimization molecular potentials for atomistic simulation studies (COMPASS) module in the Materials Studio software was used to conduct force field computations. The COMPASS force field has been parametrized for the common organic and inorganic materials using *ab initio* computations of model compounds and optimized via condensed-phase properties of polymers and low-molecular-weight compounds.<sup>21–23</sup>

In general, the total potential energy calculated in the COMPASS force field includes the following terms<sup>24</sup>

$$E_{\text{total}} = E_{\text{valence}} + E_{\text{nonbond}} \quad (1)$$

$$E_{\text{valence}} = E_{\text{diagonal}} + E_{\text{off-diagonal}} \quad (2)$$

$$E_{\text{diagonal}} = E_{\text{bond}} + E_{\text{angle}} + E_{\text{torsion}} + E_{\text{oop}} \quad (3)$$

$$E_{\text{off-diagonal}} = E_{\text{bond-bond}} + E_{\text{bond-angle}} + E_{\text{angle-angle}} + E_{\text{angle-torsion}} + E_{\text{bond-torsion}} \quad (4)$$

$$E_{\text{nonbond}} = E_{\text{coulumb}} + E_{\text{vdW}} \quad (5)$$

The valence component energy,  $E_{\text{valence}}$ , includes diagonal cross coupling terms,  $E_{\text{diagonal}}$ , and the off-diagonal cross coupling terms,  $E_{\text{off-diagonal}}$ . The diagonal term can be further decomposed into the bond stretching energy,  $E_{\text{bond}}$ , angle energy,  $E_{\text{angle}}$ , torsion energy,  $E_{\text{torsion}}$ , and out-of-plane deformation energy,  $E_{\text{oop}}$ . The off-diagonal cross coupling term,  $E_{\text{off-diagonal}}$ , includes bond–bond interaction,  $E_{\text{bond-bond}}$ , bond–angle interaction,  $E_{\text{bond-angle}}$ , angle–angle interaction,  $E_{\text{angle-angle}}$ , angle–torsion,  $E_{\text{angle-torsion}}$ , and bond–torsion interaction,  $E_{\text{bond-torsion}}$  (including central bond-torsion and terminal bond-torsion interaction). Nonbond potential energy term,  $E_{\text{nonbond}}$ , includes the Coulombic electrostatic interaction,  $E_{\text{coulumb}}$ , and the van der Waals energy of the Lennard-Jones 9-6 function,  $E_{\text{vdW}}$ .

Here, we carried out each MD simulation such a long time that we can observe several cycles of thermal vibration. The interval of each MD simulation step was typically 1 fs. All calculations were carried out at the initial temperature of 298 K except for some special conditions and NVT ensembles, in which the number of particles  $N$ , the volume  $V$ , and the temperature  $T$  can be set to desired values, were used in the calculations. In this study, the Andersen thermostat was used to control the temperature. The MD simulations with this method can produce appropriate results. We explored the simulations with undefined boundary infinite, which means that the simulated volume is infinite. To simulate the interaction between the SWNTs and PPA in the infinite volume, a MD simulation model was established with PPA molecule initially placed at the side of SWNT within the cutoff distance of 9.5 Å of van

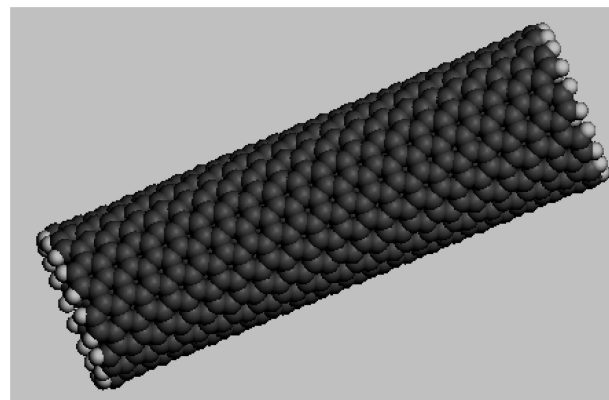


Figure 1. Molecular model of a (10, 10) SWNT.

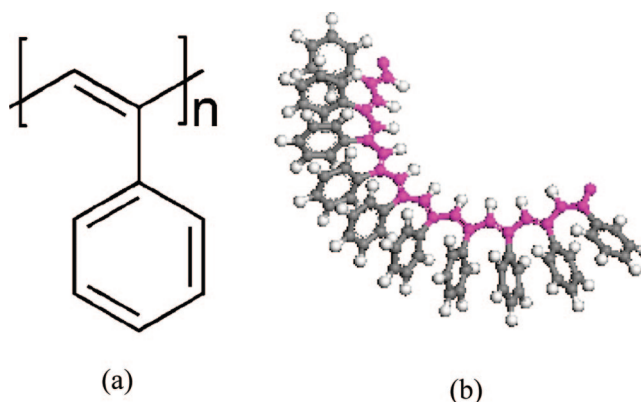


Figure 2. Chemical structure and molecular model of PPA.

der Waals interactions, and subsequently the PPA chain moved toward the surface of nanotube due to the attractive force between the PPA chain and SWNT. If the simulation time were long enough, then the polymer would move away eventually and very likely never interact with the SWNT again, which is the direct consequence of the fact that we use no boundary conditions. However, within our simulation time, the probability of this phenomenon was extremely rare, and the infinite volume does not affect the simulated results.<sup>18</sup>

### 2.2. Molecular Models. 2.2.1. Molecular Model of SWNT.

In this study, the molecular models of SWNTs with different chiralities and four kinds of chemical modifications were established by using Materials Studio. The electronic structures of carbon atoms in the SWNT models were  $sp^2$  hybridization. The unsaturated boundary effect was avoided by adding hydrogen atoms at the ends of the SWNTs. Each C–C bond length was 1.42 Å, and each C–H bond length was 1.14 Å. The hydrogen atoms had charges of +0.1268 e, and the carbon atoms connected to hydrogen atoms had charges of −0.1268 e, thus the neutrally charged SWNTs were constructed. The computer graphics picture of a (10, 10) SWNT model (with 400 carbon atoms and 40 hydrogen atoms) is shown in Figure 1.

To explore the influence of chirality, eight types of SWNTs with different chiralities were built for simulations. To assess the effect of surface modification of SWNTs on the interaction energy between the SWNTs and PPA, the functional groups, including methyl, phenyl, hydroxyl, and −F, were covalently attached to the outer surface of the (10, 10) SWNTs, which are able to modify the stacking and solvation properties of nanotubes. The functional groups were attached to the outer wall of SWNTs homogeneously and the concentrations of functionalized atoms are 7.5%.

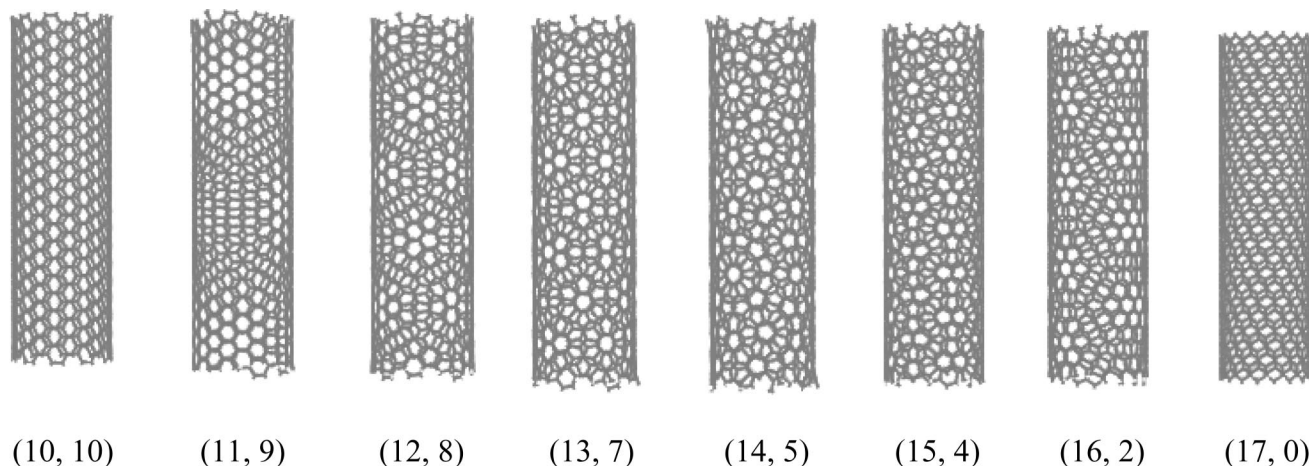


**Figure 3.** Schematics of different chiral nanotubes.

**TABLE 1: Total Number of Atoms, Diameter, and Length of Each Chiral Nanotube Utilized in MD Simulations**

type of SWNT	H atoms	C atoms	CNT diameter, Å	CNT length, Å	chiral angle $\theta$ , deg
(10, 10)SWNT armchair	40	800	13.56	49.19	30.00
(11, 9)SWNT	40	806	13.58	49.19	26.71
(12, 8)SWNT	40	808	13.65	49.19	23.43
(13, 7)SWNT	40	816	13.76	49.19	20.18
(14, 5)SWNT	38	770	13.36	49.19	14.71
(15, 4)SWNT	38	844	13.58	49.19	11.52
(16, 2)SWNT	36	820	13.38	49.19	5.82
(17, 0)SWNT zigzag	34	816	13.31	49.19	0.00

**2.2.2. Molecular Model of the PPA.** The polymer used in the simulations was PPA. A chemical structure of PPA and its molecular model comprising ten unites of phenylacetylene are shown in parts a and b of Figure 2, respectively. Energy-minimization MM was performed using Materials Studio to find the thermal stable morphology and achieve a conformation with minimum potential energy for PPA molecule. This minimum energy conformation of the molecule was used as initial status in the following MD simulations. As shown in Figure 2b, the molecular chain of PPA was twisted to achieve a low potential energy.

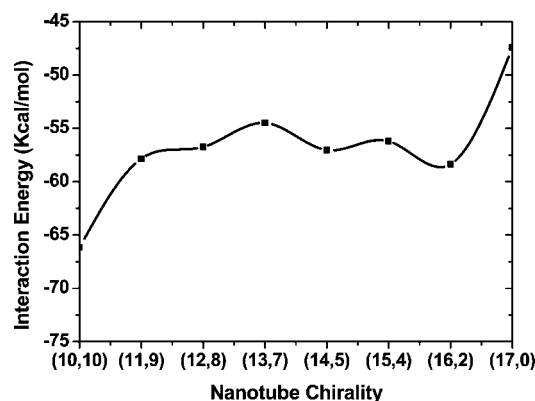
### 3. Results and Discussion

**3.1. Influence of the Nanotube Chirality on SWNT–PPA Adhesion.** To determine the influence of the nanotube chirality on SWNT–polymer adhesion, eight types of SWNTs, with different chiral angles  $\theta$  ranging from 0 to 30°, are generated,

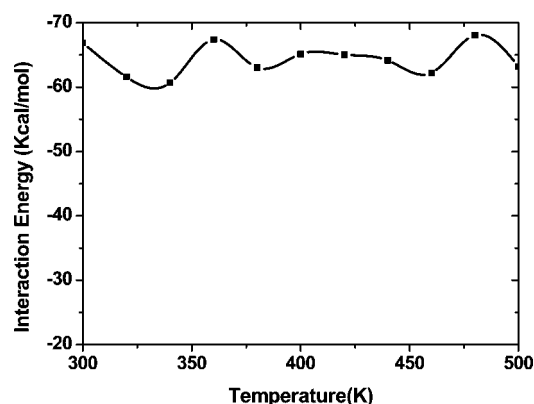
as shown in Figure 3. The corresponding chiral angle  $\theta$  and diameter  $D_n$  of SWNT with  $(n, m)$  indices could be determined by using the rolling grapheme model<sup>25</sup>

$$\theta = \arctan\left(\frac{\sqrt{3}m}{2n+m}\right) \quad D_n = \frac{\sqrt{3}}{\pi}b\sqrt{(n^2+m^2+nm)} \quad (0 \leq m \leq n) \quad (6)$$

where  $b$  is the C–C bond length (0.142 nm). The total number of atoms, diameter, and length of each chiral nanotube are presented in Table 1. The simulations were performed for 200 ps with the step of 1 fs. The first 100 ps of the simulations were carried out long enough for PPA to wrap SWNT fully and another 100 ps for data collections. All the interaction energy between SWNTs and PPA was sampled by averaging the results over the last 100 ps. Interaction energy between the SWNTs and PPA was studied using the following methodology. The interaction energy  $\Delta E$  between the nanotubes and PPA

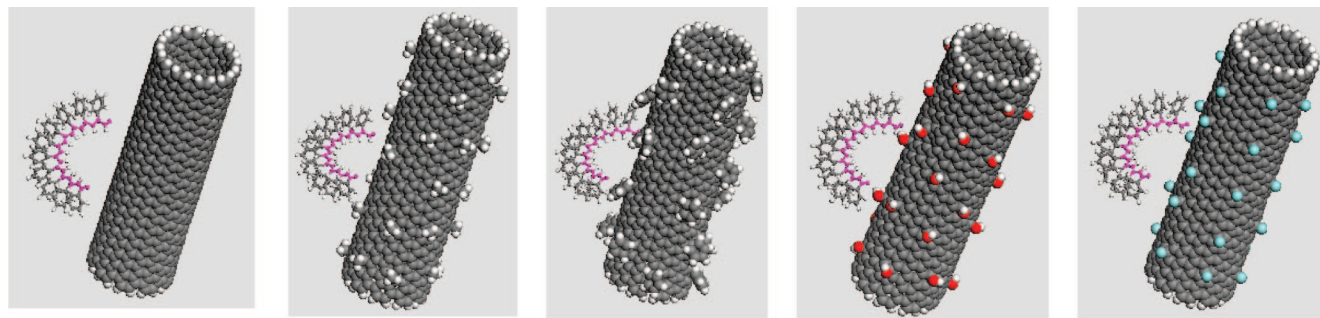


**Figure 4.** Interaction energy between the different chiral nanotubes and PPA chains.

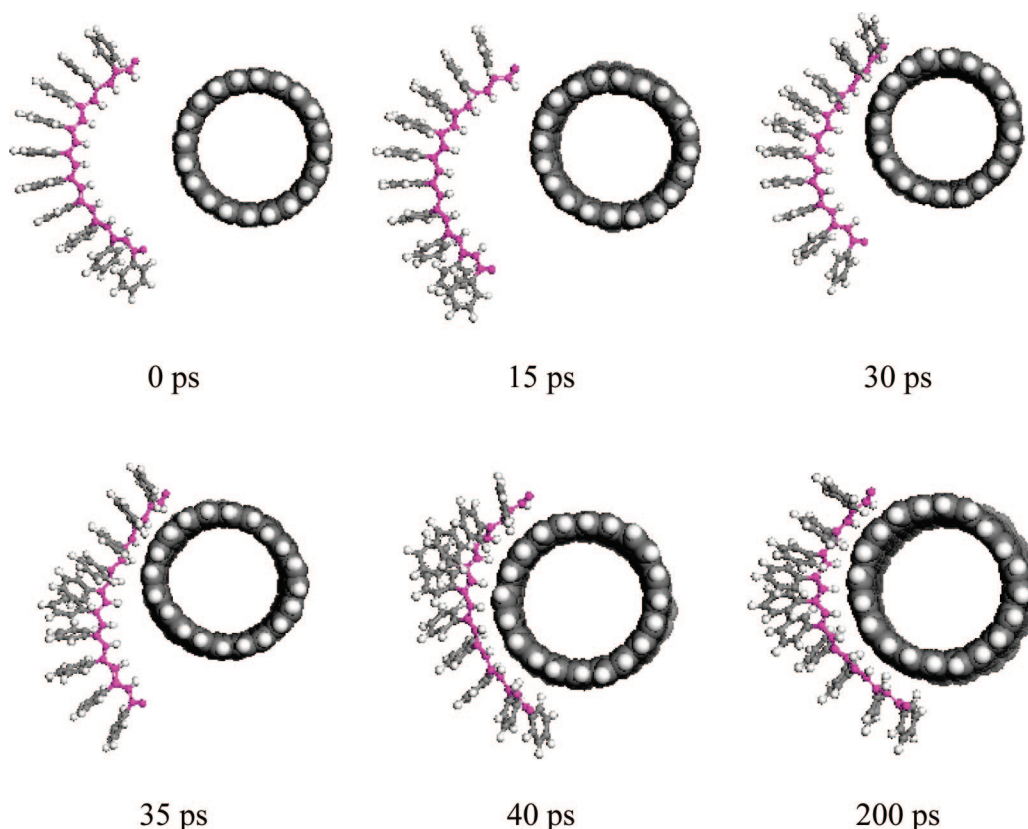


**Figure 5.** Intermolecular interaction as a function of temperature.



Unfunctionalized  
SWNT-PPAMethylic SWNT-  
PPAPhenyllic SWNT-  
PPAHydroxyl SWNT-  
PPA

-F SWNT-PPA

**Figure 6.** Side view pictures showing the initial conformations of the SWNTs and PPA molecules.**Figure 7.** MD simulation snapshots of the interactions between the PPA and unfunctionalized nanotube.

for each chiral nanotube was estimated as follows:

$$\Delta E = E_{\text{total}} - (E_{\text{CNT}} + E_{\text{PPA}}) \quad (7)$$

where  $E_{\text{total}}$  is the total energy of the system including nanotube and PPA,  $E_{\text{CNT}}$  is the energy of the isolated nanotube, and  $E_{\text{PPA}}$  is the energy of the PPA without the nanotube. In other words, the interaction energy can be calculated as the difference between the minimum energy and the energy at an infinite separation of the nanotube and the polymer matrix.<sup>26</sup> The nanotube chirality dependence of the intermolecular interaction was shown in Figure 4. It was shown that the nanotube chirality has an important effect on the attractive interaction energy between the simulated SWNTs and PPA. For armchair SWNT the attractive interaction energy is about  $-67$  kcal/mol, for zigzag SWNT it is about  $-47$  kcal/mol, while for the other chiral SWNTs it is varied between  $-47$  and  $-67$  kcal/mol. Accord-

ingly, the armchair nanotube is the best structure to interact with PPA. In the following studies, we considered SWNTs in the armchair configuration.

**3.2. Influence of the Temperature on the Interaction Energy between the SWNTs and PPA.** To assess the temperature dependence of interaction energy between the SWNTs and PPA, some MD simulations were carried out at different temperatures. The temperature was varied from 300 to 500 K with the step of 20 K. Here, the simulations were performed for 200 ps. The interaction energy was also estimated from eq 7. The average of the results was taken as the outcome. Figure 5 shows the temperature dependence of the molecular interaction energy. It was seen that the temperature has a negligible influence on the interaction between the SWNT and PPA. The variation of the interaction energy was less than 8 kcal/mol.

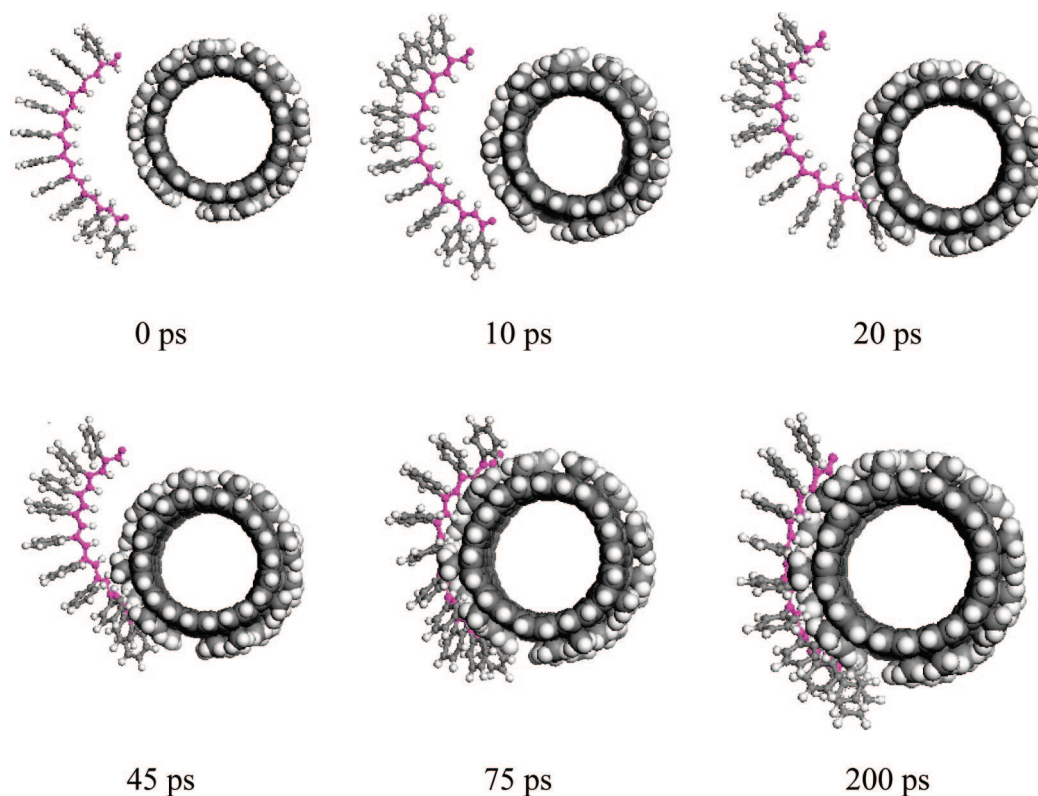


**Figure 8.** MD simulation snapshots of the interaction between the PPA and methylic nanotube.

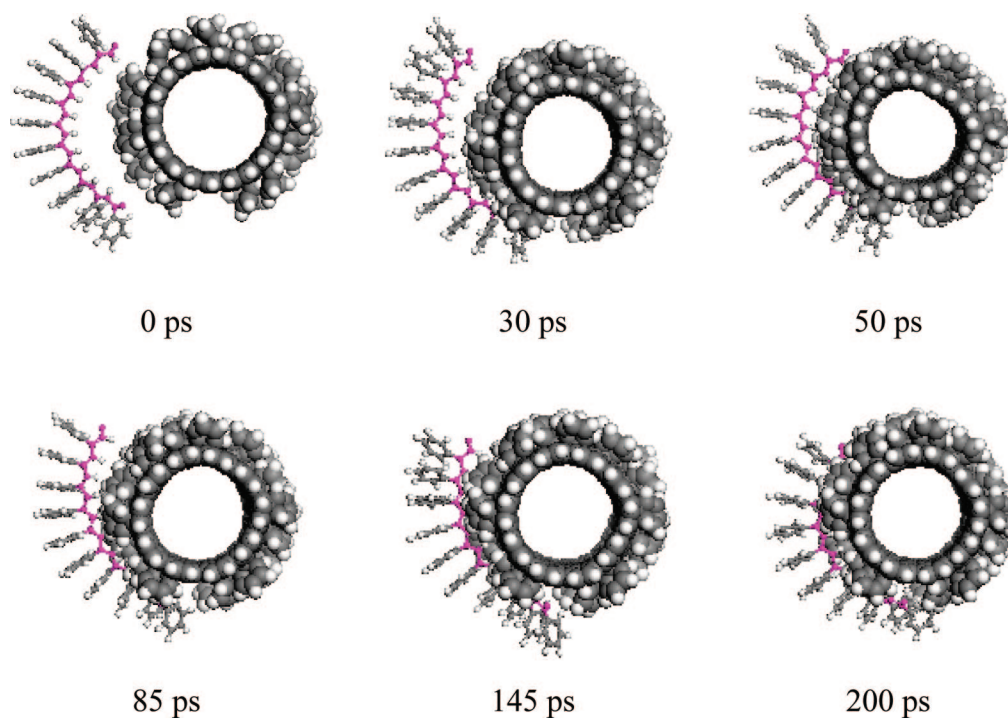


**Figure 9.** MD simulation snapshots of the interaction between the PPA and phenylic nanotube.

**3.3. Influence of Surface Chemical Modification.** The systems composed of SWNTs (five types including unmodified SWNT, methylic SWNT, phenylic SWNT, hydroxyl SWNT, and  $-F$  SWNT) and PPA, whose initial conformations were shown on the side view in Figure 6, were carried out respectively using MD simulations. Initially, all the systems were simulated for 200 ps to explore the interaction between the SWNTs and PPA. But both the hydroxyl and  $-F$  systems seemed not to reach the equilibrium state within 200 ps. The simulated time

was prolonged to 1000 ps so that it is long enough to make these systems arrive at the equilibrium state. The MD simulations of cross-section views of the interaction between the SWNTs and PPA are shown in Figures 7–11. The results showed that the molecular chains of the PPA were stretching and moving to wrap the nanotubes which were unmodified and modified by methyl or phenyl groups. Besides, we find that the PPA chains have been wrapped into the methyl or phenyl groups in the composites with SWNTs modified by methyl or phenyl



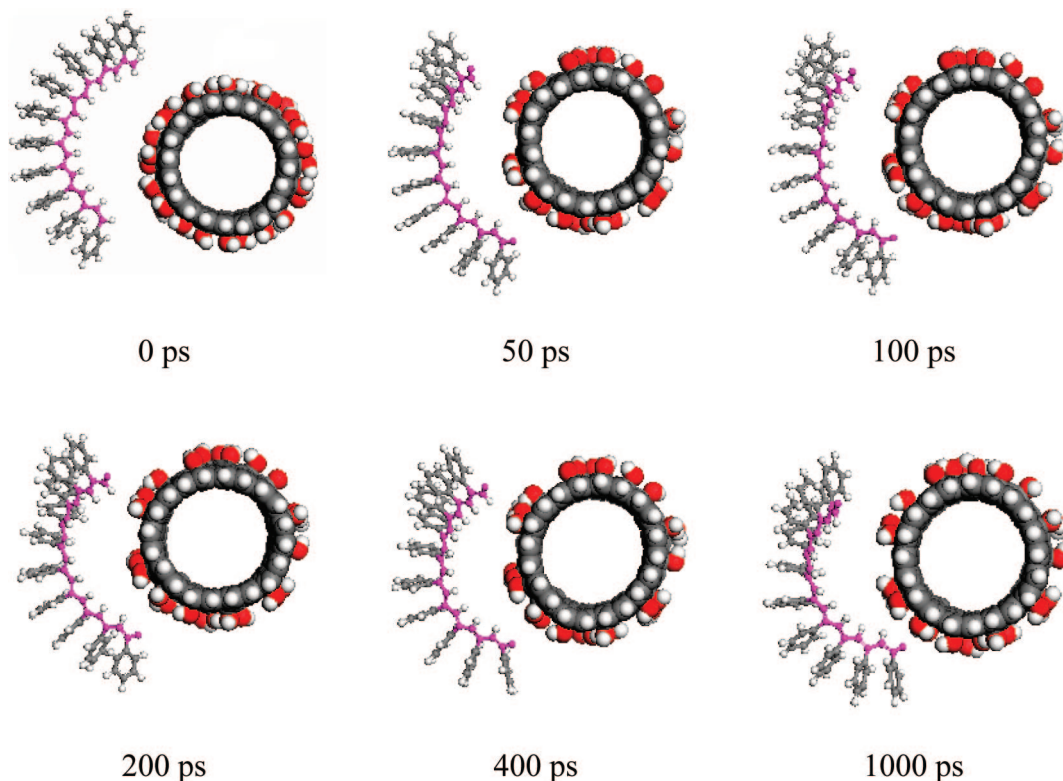


**Figure 10.** MD simulation snapshots of the interaction between the PPA and hydroxyl nanotube.

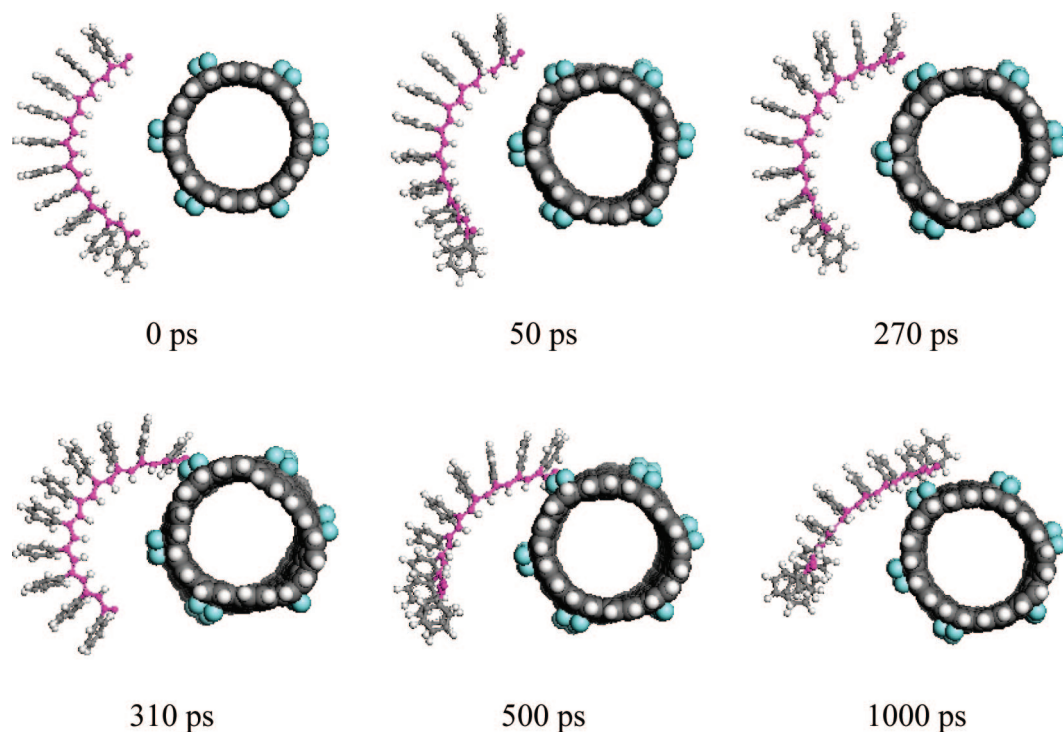


**Figure 11.** MD simulation snapshots of the interaction between the PPA and  $-F$  nanotube.

groups. In other words, it is very difficult to glide relatively and separate the PPA chains and the SWNTs modified by methyl or phenyl groups. However, the PPA chains could not move obviously to wrap the SWNTs modified by hydroxyl or  $-F$  groups even though these systems were performed for 1000 ps. Our simulations indicated that some specific chemical modifications of SWNTs play a very important role in determining the interaction strength between SWNTs and PPA. The possible

reason is that the electronic structures of the atoms of methyl or phenyl groups are more similar to that of PPA atoms.

The dynamic wrapping behavior of the PPA chain can be illustrated by tracking the interaction energy between the SWNT and PPA within the wrapping simulation time. Figure 12 shows the interaction energy between PPA and five types of SWNTs during the wrapping process. Initially, the interaction energy between the SWNTs and polymer chains for all the systems

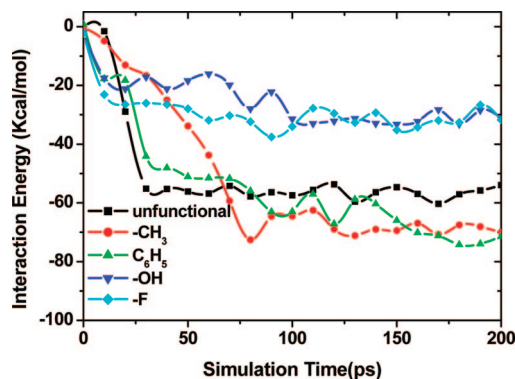


**Figure 12.** Interaction energy evolution for the five types of SWNT-PPA composites during 200 ps of wrapping simulations.

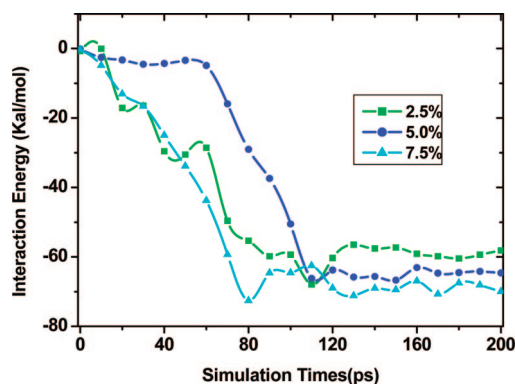


**Figure 13.** Interaction energy evolution between the methylic SWNTs (methyl groups at 2.5, 5, and 7.5% concentration) and PPA chains during 200 ps of wrapping simulations.

gradually increases. For methylic and phenylic SWNTs the absolute attractive interaction energy increases to  $-70$  kcal/mol, which is much stronger than that of the unmodified SWNTs, while for hydroxyl and  $-F$  SWNTs the absolute attractive interaction energy increases to  $-30$  kcal/mol, which is much weaker. The electronic structures of the atoms of methyl or phenyl groups are more similar to that of PPA atoms. So, it is easy for them to approach or insert into PPA chains and the interaction energy between the SWNTs and PPA may be greatly influenced by these groups.

Yang et al. demonstrated that the covalent functionalization can introduce atomic defects and weaken the CNT mechanically,<sup>27</sup> but it may not be too bad as the simulations indicate that methyl groups even at high concentrations lead only to a slight to moderate decrease in nanotube tensile strength.<sup>27</sup> Figure 13 shows the attractive energy with the simulation times for SWNTs-PPA with different concentration of methyl groups. It indicated that the interaction energy between the SWNT and PPA increases with the increase of functionalized groups' concentration. Thus, it is a tradeoff between reduced CNT strength and improved interfacial bonding. The interaction between the SWNT and PPA may be greatly influenced not only by the kinds of functionalized groups but also the concentration of functionalized groups.

#### 4. Conclusions

In this study, some MD simulations with a COMPASS force field were carried out to investigate the adhesion energy between various SWNTs and PPA chains in vacuum. The simulation results revealed that the interaction between the SWNTs and PPA is strongly influenced by the nanotube chirality while the

influence by temperature could be negligible. The MD simulations also indicated that some specific chemical modifications of SWNTs have strong influence on the interaction between the SWNTs and PPA. The SWNTs attached by methyl or phenyl groups could be well-wrapped by PPA while the others could not, which revealed that the attachment of the methyl or phenyl groups to SWNTs is beneficial to the interaction between the SWNTs and PPA, and can be effective to prevent the SWNTs from slipping in the composites. The results theoretically demonstrated the possibility of enhancing the interaction between SWNTs and polymer by selective chemical modifications of SWNTs. Our simulations also revealed that the interaction between SWNT and polymer increases with the increase of functionalized groups' concentration. Therefore, the attachment of methyl or phenyl groups with reasonable concentration to the outer SWNTs should significantly improve the load transfer between the SWNTs and polymer when the SWNTs are used to produce nanocomposites.

**Acknowledgment.** This work was supported by 973 Project under Contract No. 2008CB617508 and CNPC Innovation Fund under Contract No. 06E1024.

#### References and Notes

- (1) Iijima, S. *Nature* **1991**, *354*, 56.
- (2) Thostenson, E. T.; Ren, Z.; Chou, T. W. *Compos. Sci. Technol.* **2001**, *61*, 1899.
- (3) Ruan, S. L.; Gao, P.; Yang, X. G.; Yu, T. X. *Polymer* **2003**, *44*, 5643.
- (4) Ren, Y.; Li, F.; Cheng, H. M.; Liao, K. *Carbon* **2003**, *41*, 2177.
- (5) Andrews, R.; Weisenberger, M. C. *Curr. Opin. Solid State Mater. Sci.* **2004**, *8*, 31.
- (6) Lau, K.; Hui, D. *Composites Part B* **2002**, *33*, 263.
- (7) Du, F.; Scogna, R. C.; Zhou, W.; Brand, S.; Fischer, J. E.; Winey, K. I. *Macromolecules* **2004**, *37*, 9048.
- (8) Kymakis, E.; Alexandou, I.; Amaratunga, G. A. *J. Synth. Met.* **2002**, *127*, 59.
- (9) Biercuk, M. J.; Llaguno, M. C.; Radosavljevic, M.; Hyun, J. K.; Fischer, J. E.; Johnson, A. T.; Fischer, J. E. *Appl. Phys. Lett.* **2002**, *80*, 2767.
- (10) Wei, C. Y.; Srivastava, D.; Cho, K. J. *Nano Lett.* **2002**, *2*, 647.
- (11) Pham, J. Q.; Mitchell, C. A.; Bahr, J. L.; Tour, J. M.; Krishnamoorti, R.; Green, P. F. *J. Polym. Sci., Part B* **2003**, *41*, 3339.
- (12) Kymakis, E.; Amaratunga, G. A. *J. Appl. Phys. Lett.* **2002**, *80*, 112.
- (13) Bower, C.; Rosen, R.; Jin, L.; Han, J.; Zhou, O. *Appl. Phys. Lett.* **1999**, *74*, 3317.
- (14) Gou, J. H.; Minaie, B.; Wang, B. *Comput. Mater. Sci.* **2004**, *31*, 225.
- (15) Kuzmany, H.; Kukovecz, A.; Simon, F.; Holzweber, M.; Kramberger, C.; Pichler, T. *Synth. Met.* **2004**, *141*, 113.
- (16) Kitano, H.; Tachimoto, K.; Anraku, Y. *J. Colloid Interface Sci.* **2007**, *306*, 28.
- (17) Wei, H. F.; Hsiue, G. H.; Liu, C. Y. *Compos. Sci. Technol.* **2007**, *67*, 1018.
- (18) Yang, M. J.; Koutsos, V.; Zaiser, M. *J. Phys. Chem. B* **2005**, *109*, 10009.
- (19) Gou, J. H.; Liang, Z. Y.; Zhang, C.; Wang, B. *Composites Part B* **2005**, *36*, 524.
- (20) Frankland, S. J. V.; Caglar, A.; Brenner, D. W.; Griebel, M. J. *Phys. Chem. B* **2002**, *106*, 3046.
- (21) *Materials Studio, User's Manual, Version 1.2*; Accelrys, Inc.: San Diego, CA, 2001.
- (22) Maple, J. R.; Hwang, M. J.; Stockfisch, T. P.; Dinur, U.; Waldman, M.; Ewig, C. S.; Hagler, A. T. *J. Comput. Chem.* **1994**, *15*, 162.
- (23) Sun, H. J. *Comput. Chem.* **1994**, *15*, 752.
- (24) Liang, Z. Y.; Gou, J. H.; Zhang, C.; Wang, B.; Kramer, L. *Mater. Sci. Eng., A* **2004**, *365*, 228.
- (25) Al-Haik, M.; Hussaini, M. Y.; Garmestani, H. *J. Appl. Phys.* **2005**, *97*, 074306.
- (26) Zheng, Q. B.; Xue, Q. Z.; Yan, K. Y.; Hao, L. Z.; Li, Q.; Gao, X. L. *J. Phys. Chem. C* **2007**, *111*, 4628.
- (27) Yang, M.; Koutsos, V.; Zaiser, M. *Nanotechnology* **2007**, *18*, 155708.